

## Mixed $\beta^2/\beta^3$ -Hexapeptides and $\beta^2/\beta^3$ -Nonapeptides Folding to (*P*)-Helices with Alternating Twelve- and Ten-Membered Hydrogen-Bonded Rings

by Magnus Rueping<sup>1</sup>), Jürg V. Schreiber<sup>1</sup>), Gérald Lelais<sup>2</sup>), Bernhard Jaun\*, and Dieter Seebach\*

Laboratorium für Organische Chemie der Eidgenössischen Technischen Hochschule, ETH-Hönggerberg, Wolfgang-Pauli-Strasse 10, CH-8093 Zürich

Dedicated to Professor *James R. Bull* on the occasion of his retirement from the *Mally* Chair of Organic Chemistry at the University of Cape Town

---

The structural properties of four mixed  $\beta$ -peptides with alternating  $\beta^2/\beta^3$ - or  $\beta^3/\beta^2$ -sequences have been analyzed by two-dimensional homonuclear <sup>1</sup>H-NMR- and CD spectroscopic measurements. All four  $\beta$ -peptides fold into (*P*)-helices with twelve- and ten-membered H-bonded rings (Figs. 3–6). CD Spectra (Fig. 2) of the mixed  $\beta^3/\beta^2$ -hexapeptide **4a** and  $\beta^3/\beta^2$ -nonapeptide **5a**, indicating that peptides of this type also adopt the *12/10*-helical conformation, were confirmed by NMR structural analysis. For the deprotected  $\beta^3/\beta^2$ -nonapeptide **5d**, NOEs not consistent with the *10/12* helix have been observed, showing that the stability of the helix decreases upon N-terminal deprotection. From the NMR structures obtained, an idealized helical-wheel representation was generated (Fig. 7), which will be used for the design of further *12/10* or *10/12* helices.

---

**1. Introduction.** – Many synthetic oligomers with conformations similar to those of natural peptides and proteins have recently been studied [1]. Considerable attention has been drawn to peptides consisting of  $\beta$ - and  $\gamma$ -amino acids, especially as it was shown that  $\beta$ - and  $\gamma$ -peptides can be designed to fold into secondary structures analogous to those found in proteins [2–6]. Since these homologous oligomers are structurally related to  $\alpha$ -peptides, their investigation might deepen our understanding of protein folding. Like  $\alpha$ -peptides,  $\beta$ - and  $\gamma$ -peptides contain amide groups that are able to form intra- and intermolecular H-bonds to generate helices, turns, and sheets.

Short-chain  $\beta$ -peptides containing six or seven residues form various stable helices in organic and aqueous solutions. Apart from *14*- [7–17], *12*- [18][19], and *10*-helical [20] structures and a ribbon-type arrangement of eight-membered H-bonded rings [21], another type of helix, a right-handed *12/10*-helix [22][23] (Fig. 1) was identified when an unprotected ‘mixed’  $\beta$ -peptide containing both  $\beta^2$ - and  $\beta^3$ -amino acids was analyzed by NMR spectroscopy in pyridine and MeOH solutions.

The structure of this (*P*)-*12/10*-helix is characterized by alternating wide twelve-membered and narrow ten-membered H-bonded rings with the amide groups pointing alternatively up and down the helix axis, resulting in a smaller dipole of the *12/10*-helix compared to other helical conformations. The structural analysis further revealed that conformationally restricted amide bonds with two neighboring substituents (between

---

<sup>1</sup>) Part of the Ph.D. theses of *M. R.* (ETH-Zürich, Diss. No. 14677) and *J. V. S.* (ETH-Zürich, Dissertation No. 14298).

<sup>2</sup>) Part of the projected Ph.D. thesis of *G. L.*, ETH-Zürich.

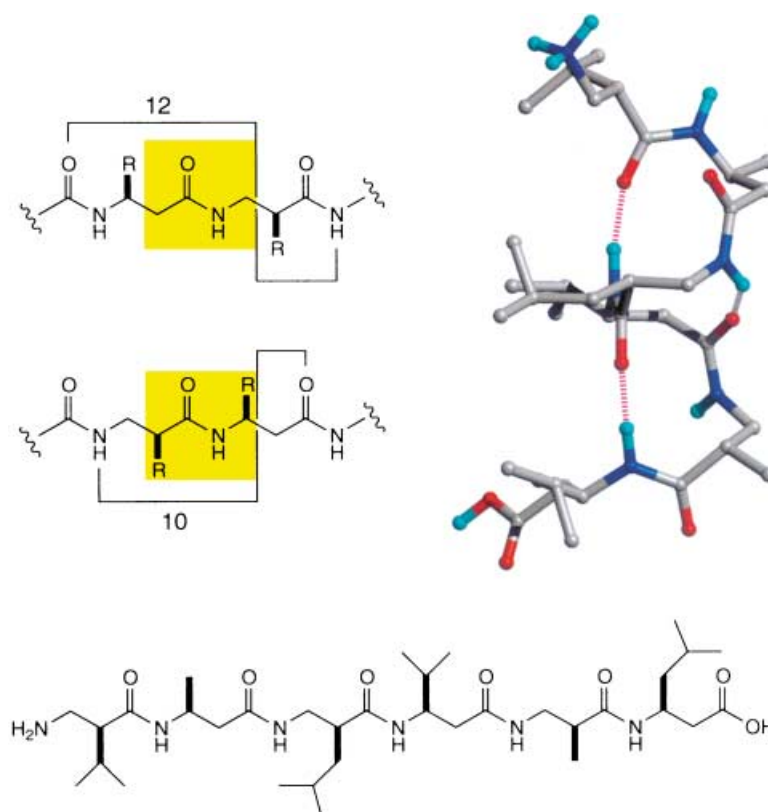


Fig. 1. Model of a (P)-12/10-helix. The helix is characterized by alternating wide twelve-membered and narrow ten-membered rings with the C=O groups pointing alternatively up and down the helix axis (right). The amide bonds in  $\beta$ -peptides, consisting of alternating  $\beta^2$ - and  $\beta^3$ -amino acids, which are flanked by unsubstituted C-atoms, induce twelve-membered H-bonded rings, while the amide bonds with flanking substituents induce ten-membered H-bonded rings (left).

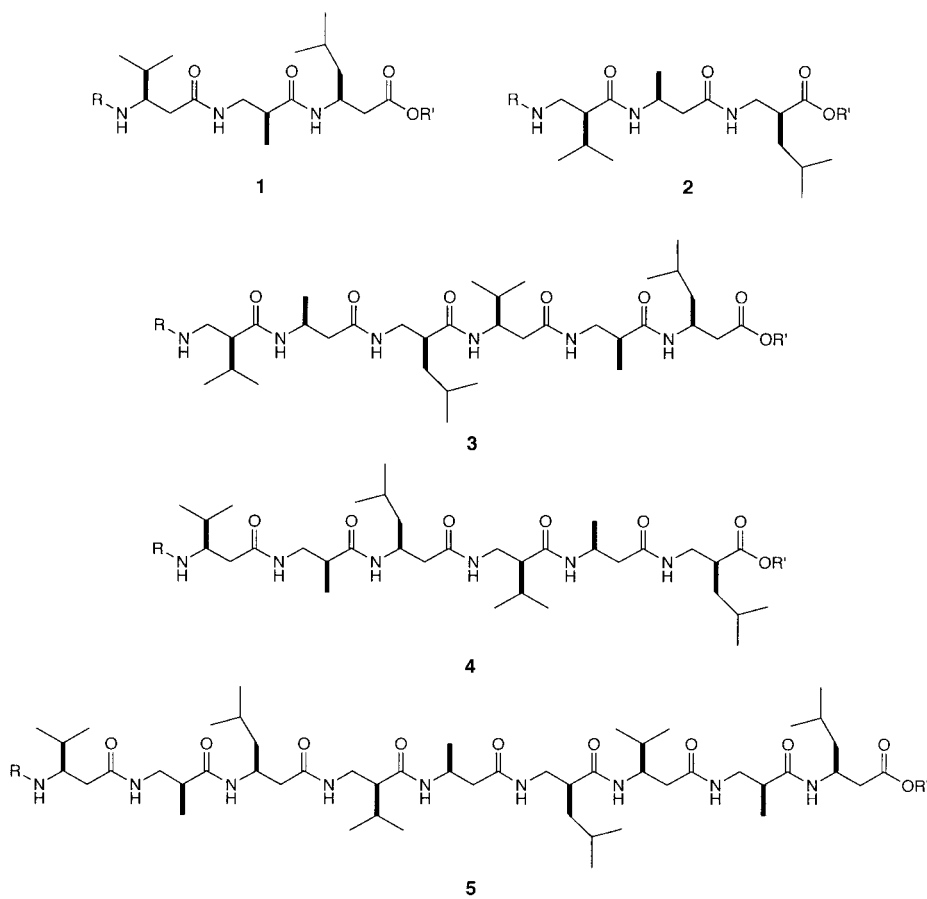
residue 1 and 2, 3 and 4, and 5 and 6) induce the formation of ten-membered H-bonded rings<sup>3)</sup>, while the amide bonds with no adjacent substituents prefer twelve-membered H-bonded rings (Fig. 1). In addition to the NMR investigations of the unprotected hexapeptide, molecular-mechanics<sup>4)</sup> [27–29] and molecular-dynamics calculations [30][31] were performed, and the latter showed reversible folding to the experimentally determined right-handed 12/10-helix. A complete 12/10/12-helix was sampled at various times in the simulation. Also 14-membered rings occurred around 1–3% of the time and a  $3_{14}$ -helical structure was found twice during the simulation<sup>5)</sup>.

<sup>3)</sup> The ten-membered H-bonded ring was also used for the design of the central part of a  $\beta$ -peptidic hairpin [24] and of  $\beta$ -peptidic turns [25][26].

<sup>4)</sup> *Ab initio* quantum-mechanics calculations showed that the preference for the 12/10-helix over other helical conformations is dependent on the side chains and side-chain substitution pattern, in agreement with the experimental observations.

<sup>5)</sup> This finding was consistent with experimentally observed NOEs, which are typical of  $3_{14}$ -helical conformations [23].

To obtain more information about the folding and stability of the *12/10*-helix, the mixed  $\beta^2/\beta^3$ - and  $\beta^3/\beta^2$ -peptides **3–5** have been prepared. The protected  $\beta$ -hexapeptides **3a** and **4a**, as well as the protected and unprotected  $\beta$ -nonapeptides **5a** and **5d** have been analyzed by NMR spectroscopy to address the questions of *i*) whether replacement of the  $\beta^2/\beta^3$ - by a  $\beta^3/\beta^2$ -sequence results in a change of N-terminal ring size (ten- vs. twelve-membered ring), *ii*) whether protection of mixed peptides leads to a more stable helix<sup>6</sup>, and *iii*) whether the *12/10* ring pattern is repetitive in longer chains.



**a** R = Boc, R' = Bn

**b** R = Boc, R' = H

**c** R = H, R' = Bn, as trifluoroacetate

**d** R = R' = H, as trifluoroacetate

<sup>6</sup>) CD-Spectroscopic measurements of a protected and unprotected mixed  $\beta^2/\beta^3$ -dodecapeptide showed a collapse of the CD pattern upon deprotection [22].

**2. Preparation of the Mixed  $\beta$ -Peptides.** – The  $\beta$ -peptides **1–5** were synthesized in solution by conventional peptide-coupling methods with EDC/HOBt as coupling reagents. The fully protected  $\beta$ -tripeptides **1a** and **2a** were prepared from the corresponding  $\beta^2$ - and  $\beta^3$ -amino acids<sup>7)</sup> as previously described. The  $\beta$ -tripeptides **1a** and **2a** were either debenzylated ( $H_2/Pd-C$ ) to give **1b** and **2b** or *N*-deprotected with  $CF_3COOH$  (TFA) to furnish **1c** and **2c**. Subsequent peptide coupling of **1b** and **2b** with **2c** and **1c**, respectively, gave the fully protected  $\beta$ -hexapeptides **4a** and **3a**. Hexapeptide **3a** was *N*-Boc-deprotected with TFA and coupled with **1b** to yield the  $\beta$ -nonapeptide **5a**. Hydrogenolysis and Boc-deprotection of **5a** provided the fully deprotected  $\beta$ -nonapeptide **5d**.

**3. Structural Analysis.** – 3.1. *CD Spectroscopy.* CD Spectroscopy is frequently used to elucidate secondary structures of  $\alpha$ -peptides and proteins in solution [37]. Although, for  $\beta$ -peptides, the correlation between CD pattern and secondary structure is not yet fully established, it provides useful information when used in combination with other spectroscopic techniques. The CD spectra of the mixed  $\beta^3/\beta^2$ -peptides **4a** and **5a** were recorded in MeOH (0.2 mM) solutions and show a pattern with a single maximum at *ca.* 202 nm with the molar ellipticity  $\theta$  increasing with chain length (*Fig. 2, a*). Hence, the CD spectra are in agreement with the previously observed CD curves of  $\beta^2/\beta^3$ -hexapeptides and  $\beta^2/\beta^3$ -dodecapeptides of type **3** and indicate that longer mixed  $\beta$ -peptides also adopt the *12/10*-helical pattern. Additional spectra were recorded in the presence of helix-destabilizing urea and in acidic solutions (*Fig. 2, b and c*). Interestingly, in the case of urea addition (3M), the single maximum pattern of **4a** remains, although with lower intensity and shifted towards longer wavelength (211 vs. 202 nm). Different behavior is observed upon addition of  $MeSO_3H$ : the positive Cotton effect at 202 nm decreases rapidly in the presence of 25%  $MeSO_3H$  and completely disappears with the addition of 75%  $MeSO_3H$ <sup>8)</sup>, indicating a loss of the helical structure.

3.2. *NMR Investigations.* To obtain further information about the folding and stability of the mixed  $\beta$ -peptides, a detailed NMR-structural investigation was performed. The NMR measurements of the mixed  $\beta$ -peptides **3a–5a** and **5d** were carried out in MeOH solutions by DQF-COSY, TOCSY, HSQC, HMBC, and ROESY techniques. A full assignment of all  $^1H$  resonances of the respective amino acid spin systems and the determination of the sequences was achieved by COSY and TOCSY measurements, and for the  $\beta$ -nonapeptides, HSQC and HMBC spectra were additionally used (*Tables 1–4*).

ROESY Spectra were recorded at different mixing times (150 and 300 ms), and NOEs were collected for the spectra with a mixing time of 300 ms<sup>9)</sup>. Qualitative analysis of the different ROESY spectra showed that typical NOEs for the *12/10*- and *10/12*-helices were present for all four peptides, but, in the case of the unprotected  $\beta$ -

7) The required  $\beta^2$ - and  $\beta^3$ -amino acid derivatives were prepared by either *Arndt-Eistert* homologation [32][33] of the corresponding  $\alpha$ -amino acid or by amidomethylation [34] of a Ti-enolate of an acylated modified *Evans* auxiliary [35][36].

8) Similar observations have been made for a  $\beta^3$ -dodecapeptide [17] and the polymer  $H-(\beta-HLys(Cbz))_n-OH$  [38].

9) For a complete list of NOEs, see *Exper. Part*.

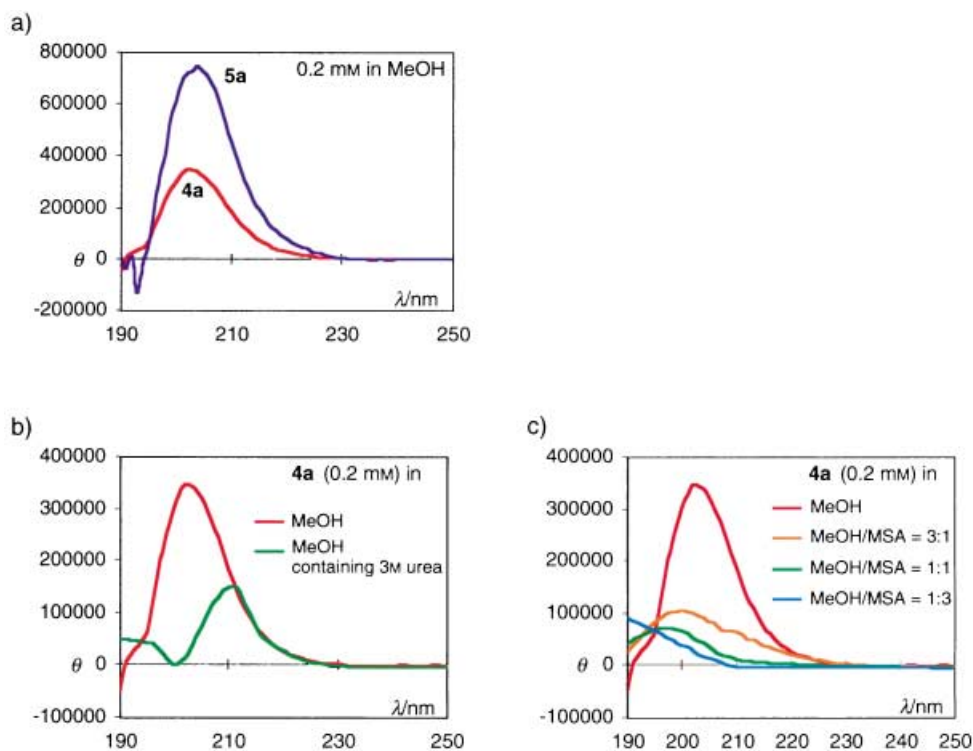


Fig. 2. a) CD Spectra of the fully protected  $\beta^3/\beta^2$ -hexapeptide and  $\beta^3/\beta^2$ -nonapeptide **4a** and **5a**, respectively, in MeOH; b) of the  $\beta^3/\beta^2$ -hexapeptide **4a** in MeOH and in MeOH containing 3M urea; and c) in the presence of increasing amounts of MSA. The spectra were recorded at room temperature, at a concentration of 0.2 mM; they are not normalized. Molar ellipticity ( $\theta$ ) in  $10^4 \text{ deg} \cdot \text{cm}^2 \cdot \text{mol}^{-1}$ .

Table 1.  $^1\text{H}$ - and  $^{13}\text{C}$ -NMR Chemical Shifts of  $\beta$ -Peptide **3a** in MeOH

$\beta$ -Amino acid	NH ( $J(\text{NH},\text{H}\beta)$ )	C=O	H-C( $\alpha$ ), 2 H-C( $\alpha$ )	H-C( $\beta$ ), 2 H-C( $\beta$ )	H-C( $\gamma$ ), 2 H-C( $\gamma$ ), Me( $\gamma$ )	H-C( $\delta$ ), Me( $\delta$ )	Me( $\epsilon$ )
Val <sup>1</sup>	6.48	175.02	2.05 45.71	3.47/313 42.29	1.80 30.05	1.01/0.93 20.75	
Ala <sup>2</sup>	8.02 (9.11 Hz)	173.67	2.59/2.10 42.05	4.55 45.39	1.22 21.47		
Leu <sup>3</sup>	8.43	176.37	2.58 45.63	3.66/2.73 43.71	1.54/1.02 39.82	1.69 25.97	0.92 20.91
Val <sup>4</sup>	8.58 (9.74 Hz)	174.26	2.53/2.14 42.04	4.24 54.77	1.77 33.85	0.96 20.27	
Ala <sup>5</sup>	7.83	176.97	2.47 41.42	3.49/2.88 44.34	1.07 15.30		
Leu <sup>6</sup>	8.50 (8.61 Hz)	174.12	2.62/2.56 45.67	4.38 46.63	1.49/1.32 27.16	1.52 25.91	0.90 21.97
Other: $^t\text{Bu}$ = 1.44, $\text{PhCH}_2$ = 5.17/5.06							

Table 2.  $^1\text{H}$ - and  $^{13}\text{C}$ -NMR Chemical Shifts of  $\beta$ -Peptide **4a** in MeOH

$\beta$ -Amino acid	NH ( $J(\text{NH},\text{H}\beta)$ )	C=O	H–C( $\alpha$ ), 2 H–C( $\alpha$ )	H–C( $\beta$ ), 2 H–C( $\beta$ )	H–C( $\gamma$ ), 2 H–C( $\gamma$ ), Me( $\gamma$ )	H–C( $\delta$ ), Me( $\delta$ )	Me( $\epsilon$ )
Val <sup>1</sup>	6.42 (10.21 Hz)	174.05	2.62/2.07 41.49	4.02 56.23	1.69 34.55	0.94 19.95	
Ala <sup>2</sup>	8.51	176.25	2.27 42.77	3.65/2.73 44.18	1.04 15.04		
Leu <sup>3</sup>	8.16 (9.35 Hz)	173.44	2.56/2.14 44.69	4.40 47.77	1.56/1.30 40.40	1.69 34.60	0.98 20.72
Val <sup>4</sup>	8.14	173.32	2.76 45.02	3.34/2.78 48.87	1.56 27.29	0.88 23.33	
Ala <sup>5</sup>	8.31	175.77	2.42/2.31 43.69	4.27 44.79	1.17 20.91		
Leu <sup>6</sup>	8.33	176.44	1.93 55.17	3.82/2.85 41.11	1.55/1.26 45.31	0.97 20.70	0.90 18.48
Other: <sup>t</sup> Bu = 1.43, PhCH <sub>2</sub> = 5.12/5.02							

Table 3.  $^1\text{H}$ - and  $^{13}\text{C}$ -NMR Chemical Shifts of  $\beta$ -Peptide **5a** in MeOH

$\beta$ -Amino acid	NH ( $J(\text{NH},\text{H}\beta)$ )	C=O	H–C( $\alpha$ ), 2 H–C( $\alpha$ )	H–C( $\beta$ ), 2 H–C( $\beta$ )	H–C( $\gamma$ ), 2 H–C( $\gamma$ ), Me( $\gamma$ )	H–C( $\delta$ ), Me( $\delta$ )	Me( $\epsilon$ )
Val <sup>1</sup>	6.33 (10.15 Hz)	174.01	2.55/1.97 41.41	3.96 56.09	1.60 34.39	0.83 19.22	
Ala <sup>2</sup>	8.42	176.35	2.17 42.68	3.57/2.60 44.14	0.94 15.12		
Leu <sup>3</sup>	8.12 (9.90 Hz)	173.51	2.61/2.08 44.93	4.47 47.83	1.50/1.23 45.06		
Val <sup>4</sup>	8.39	175.41	1.79 34.75	3.84/2.61 41.05	1.65 33.73	1.64 29.16	0.84 19.56
Ala <sup>5</sup>	8.46 (9.17 Hz)	177.04	2.55/2.04 46.29	4.51 45.56	1.13 21.66	0.87/0.78	
Leu <sup>6</sup>	8.44	176.70	2.54 43.61	3.55/2.58 43.71	1.54/1.19 30.54		
Val <sup>7</sup>	8.77 (10.21 Hz)	174.40	2.42/2.05 41.94	4.15 54.52	1.01 28.75	1.41 27.16	0.83/0.79
Ala <sup>8</sup>	7.75	173.34	2.36 41.22	3.40/2.76 44.20	0.95 15.09	0.83	
Leu <sup>9</sup>	7.42	174.22	2.52/2.44 41.94	4.26 46.21	1.40/1.20 44.37	1.61 25.95	0.87/0.80
Other: <sup>t</sup> Bu = 1.34, PhCH <sub>2</sub> = 5.09/4.97							

nonapeptide **5d**, weak NOEs not compatible with the *I0/I2*-helical structure were also present<sup>10</sup>).

Integration of the NOE cross-peak volumes, followed by calibration and classification into three distance categories, allowed their use as distance constraints

<sup>10</sup>) The three NOEs (NH<sub>(6)</sub> to H–C( $\beta$ )<sub>(3,4)</sub> and NH<sub>(2)</sub> to H–C( $\beta$ )<sub>(5)</sub>) are not consistent with all other NOEs and the *I0/I2*-helix, but indicate that other conformations must be populated, besides the *I0/I2*-helical structure, a result previously obtained by NMR investigations and MD simulations for the deprotected  $\beta^2/\beta^3$ -hexapeptide **3d** (see above). These NOEs were not considered in the simulated-annealing calculations.

Table 4.  $^1\text{H}$ - and  $^{13}\text{C}$ -NMR Chemical Shifts of  $\beta$ -Peptide **5d** in MeOH

$\beta$ -Amino acid	NH ( $J(\text{NH},\text{H}\beta)$ )	C=O	H–C( $\alpha$ ), 2 H–C( $\alpha$ )	H–C( $\beta$ ), 2 H–C( $\beta$ )	H–C( $\gamma$ ), 2 H–C( $\gamma$ ), Me( $\gamma$ )	H–C( $\delta$ ), Me( $\delta$ )	Me( $\epsilon$ )
Val <sup>1</sup>	–	172.46	2.79/2.53 35.40	3.41 56.07	1.97 31.97	1.60/1.01 n.a.	
Ala <sup>2</sup>	8.24	176.68	2.57 42.27	3.42/3.22 43.67	1.09 15.95		
Leu <sup>3</sup>	8.05 (9.54 Hz)	173.77	2.59/2.20 44.17	4.47 47.24	1.63 26.15	1.45/1.31 45.70	0.91 n.a.
Val <sup>4</sup>	8.50	175.17	2.66 45.21	3.43/2.93 43.50	1.58 40.37	0.99 18.18	
Ala <sup>5</sup>	8.45 (8.93 Hz)	177.91	2.57/2.25 45.65	4.54 45.32	1.21 21.79		
Leu <sup>6</sup>	8.47	176.45	2.05 54.73	3.64/3.01 41.10	1.78 29.90	1.68 26.13	0.94/0.87 n.a.
Val <sup>7</sup>	8.54 (9.66 Hz)	174.08	2.50/2.16 41.19	4.24 54.41	1.80 33.84	0.92 18.05	
Ala <sup>8</sup>	7.91	176.75	2.45 41.61	3.35/3.09 44.10	1.05 15.65		
Leu <sup>9</sup>	8.35 (8.68 Hz)	175.79	2.52/2.44 41.59	4.36 46.32	1.67 26.09	1.46/1.31 45.14	0.91 n.a.

n.a.: not available

in slow-cooling-simulated annealing calculations by means of the X-PLOR program. Each calculation was started from randomized conformers, and a bundle of the respective lowest-energy conformers was used to represent the NMR structures of the mixed  $\beta$ -peptides **3a**–**5a** and **5d** (Figs. 3–6). All four  $\beta$ -peptides fold into helices with alternating twelve- and ten-membered H-bonded rings. The protected  $\beta^3/\beta^2$ -peptides **4a** and **5a** (Figs. 4 and 5) adopt a helical pattern, which is characterized by a twelve-membered H-bonded ring from the C=O of the N-terminal Boc group to the NH of residue 3 and continuing ten- and twelve-membered H-bonded rings (Fig. 7). Hence, the protected  $\beta^3/\beta^2$ -peptides **4a** and **5a** form the same *12/10*-helix as the previously reported deprotected  $\beta^2/\beta^3$ -peptide **3d** (Fig. 1). In contrast, the *N*-Boc-protected  $\beta^2/\beta^3$ -peptide **3a** (Fig. 3) and the deprotected  $\beta^3/\beta^2$ -peptides **5d** (Fig. 6) fold into *10/12*-helical structures with ten-membered H-bonded rings from  $\text{NH}_{(i)}$  (**3a**,  $i=1$ ; **5d**,  $i=2$ ) to  $\text{C}=\text{O}_{(i+1)}$  and continuing twelve- and ten-membered H-bonded rings (Fig. 7). Thus, the *N*-terminal Boc protecting group participates in the formation of the first H-bonded ring, while the benzylester protecting group seems to destabilize the *C*-terminus of the helices, as shown by the less-defined *C*-termini (Fig. 3–5).

**4. Conclusions.** – Following our previous investigations of  $\beta$ -peptides consisting of alternating  $\beta^2$ - and  $\beta^3$ -amino acids, we have now analyzed protected and deprotected peptides, and peptides with longer sequences and different substitution patterns by means of high-resolution NMR techniques. In MeOH solution, all peptides fold into (*P*)-helices with alternating twelve- and ten-membered H-bonded rings, demonstrating that the alternating ring pattern is also repetitive in longer-chain analogs (Figs. 5 and 6).

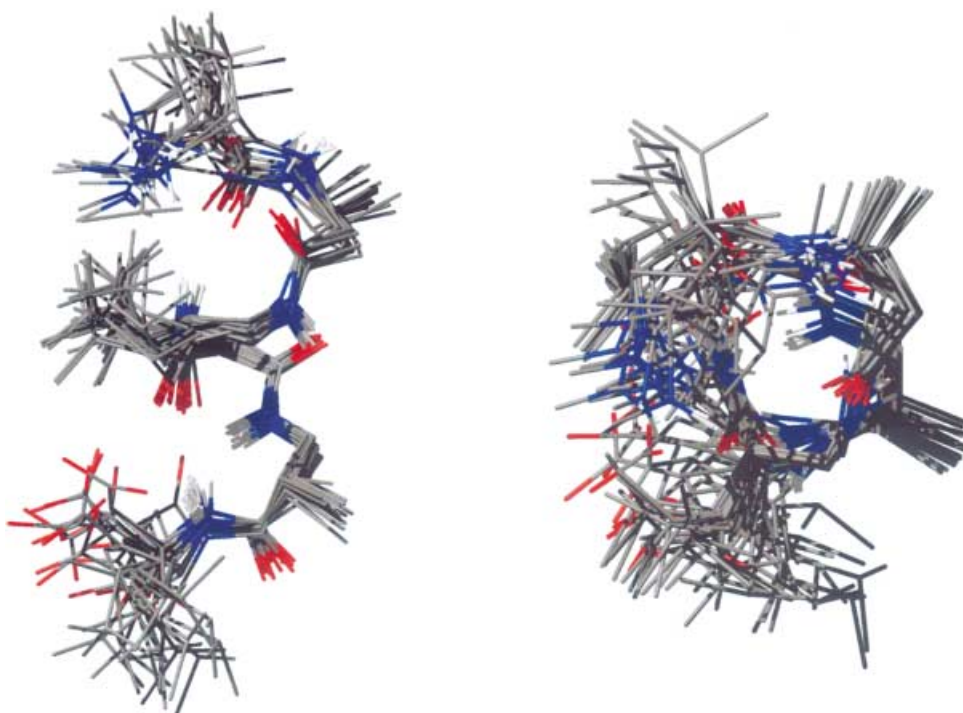


Fig. 3. NMR-Solution structure of the  $\beta^3/\beta^3$ -hexapeptide **3a** in MeOH represented by a bundle of the 20 lowest-energy structures as obtained by simulated annealing. View along the 10/12-helical axis (left) and top view (right) with the C- and N-terminal protecting groups omitted.

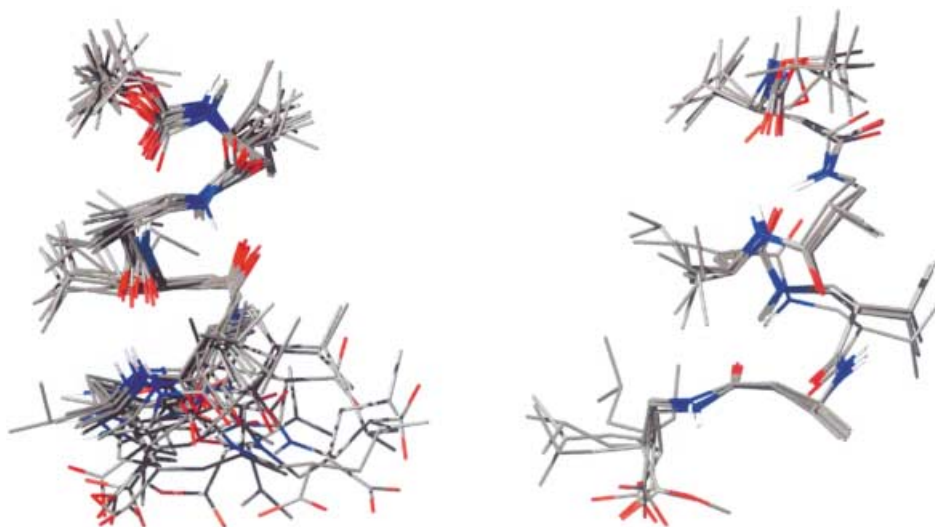


Fig. 4. NMR-Solution structure of the  $\beta^3/\beta^2$ -hexapeptide **4a** in MeOH represented by a bundle of the 12 (left) and 5 (right) lowest-energy 12/10-helical structures as obtained by simulated annealing, with the C-terminal protecting group omitted



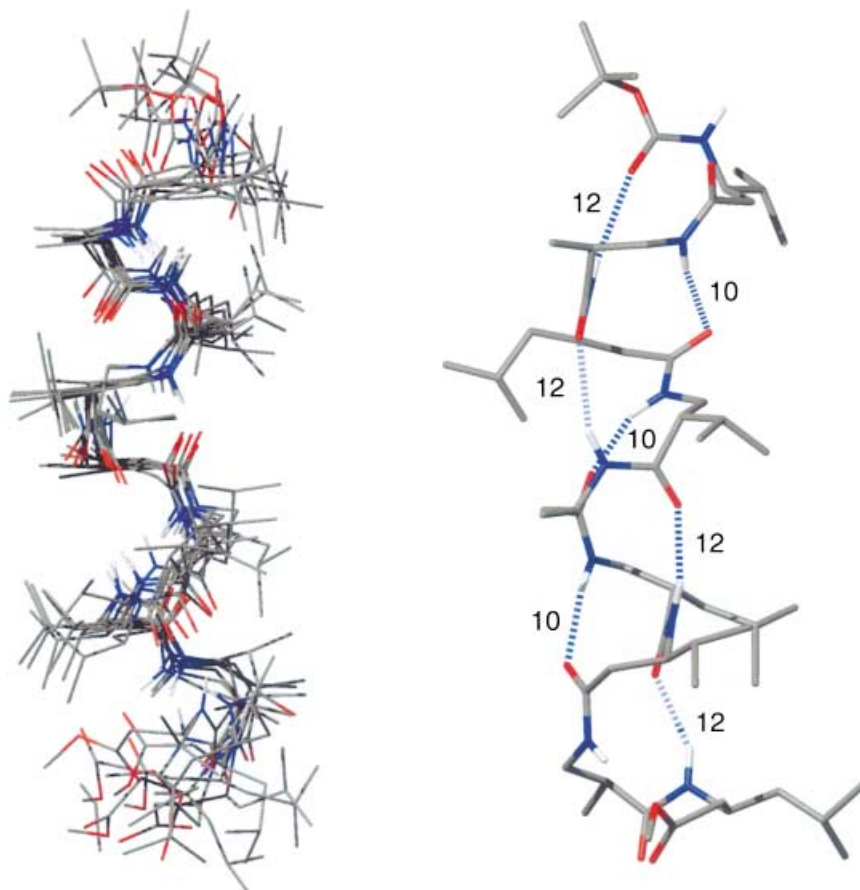


Fig. 5. NMR-Solution structure of the fully protected  $\beta^3/\beta^2$ -nonapeptide **5a** in MeOH represented by a bundle of the 10 lowest-energy structures as obtained by simulated annealing (left). A conformer with alternating twelve- and ten-membered H-bonded rings (right). The C-terminal protecting group is omitted for clarity.

However, removal of the protecting groups destabilizes the helix<sup>11)</sup>, as indicated by NOEs, which are not compatible with the helical pattern. This observation is in agreement with previous CD measurements and MD simulations. The destabilizing effect upon deprotection may be counteracted by the introduction of conformational constraints, such as disulfide bridges or side chains that are able to form salt bridges in appropriate positions (Fig. 7) on the helix.

<sup>11)</sup> This result is in contrast to the case of  $\beta^3$ -peptides, which form  $3_{14}$ -helical structures and become destabilized by N-terminal protection [8][31].

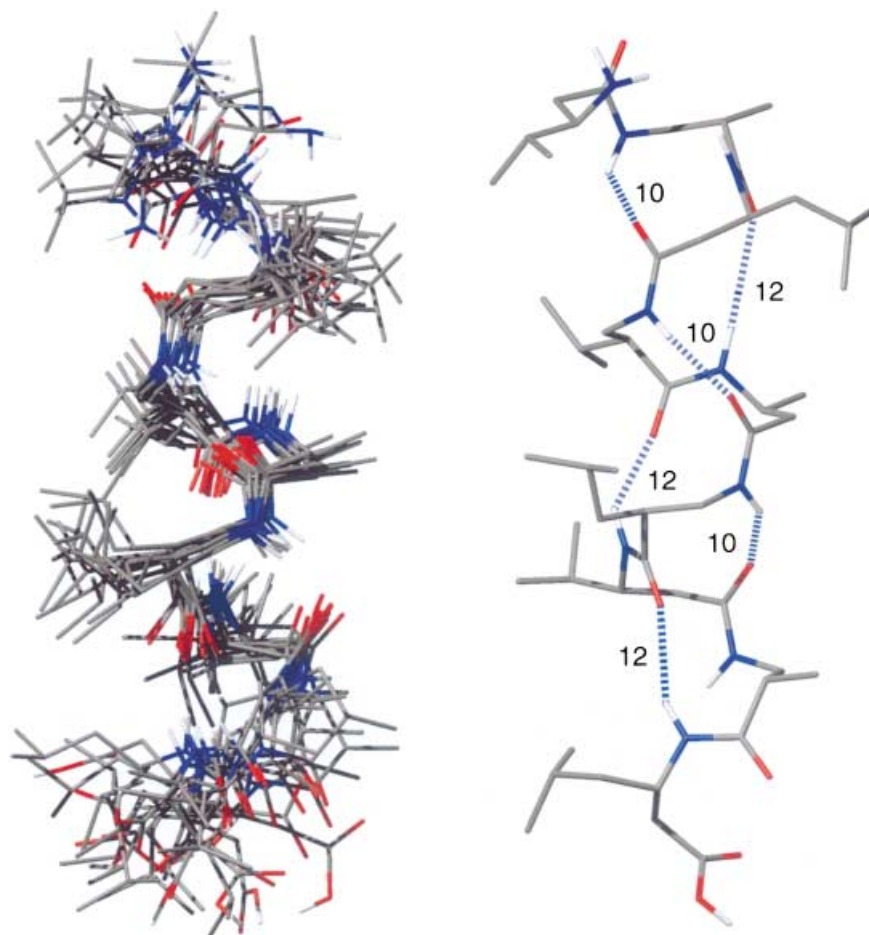


Fig. 6. NMR-Solution structure of the fully deprotected  $\beta^3/\beta^2$ -nonapeptide **5d** in MeOH represented by a bundle of the 10 lowest-energy structures as obtained by simulated annealing (left). A conformer with alternating ten- and twelve-membered H-bonded rings (right). NOEs that are not compatible with the 10/12-helix were not used in the calculation.

#### Experimental Part

1. *General. Abbreviations:* EDC: 1-[3-(dimethylamino)propyl]-3-ethylcarbodiimide hydrochloride), FC: flash chromatography, HOBt: 1-hydroxy-1H-benzotriazole), h.v.: high vacuum, 0.01–0.1 Torr, NMM: *N*-methylmorpholine. Solvents for chromatography and workup procedures were distilled from *Sikkon* (anh. CaSO<sub>4</sub>; *Fluka*). Amino acid derivatives were purchased from *Bachem*, *Degussa*, or *Senn*. All other reagents were used as received from *Fluka*. The  $\beta$ -amino acid derivatives *Boc*-(R)- $\beta^3$ -HVal-(S)- $\beta^2$ -HAla-(S)- $\beta^2$ -HLeu-OBn (**1a**), *Boc*-(S)-B<sup>2</sup>-HVal-(S)- $\beta^3$ -HAla-(S)- $\beta^2$ -HLeu-OBn (**2a**), and *Boc*-(S)- $\beta^2$ -HVal-(S)- $\beta^3$ -HAla-(S)- $\beta^2$ -HLeu-(R)- $\beta^3$ -HVal-(S)- $\beta^2$ -HAla-(S)- $\beta^3$ -HLeu-OBn (**3a**) were prepared according to literature procedures [23]. TLC: *Merck* silica-gel 60 *F*<sub>254</sub> plates; detection with UV and anisaldehyde. FC: *Fluka* silica gel 60 (40–63 mm); at ca. 0.2 bar. Anal. HPLC: *Knauer* HPLC System (pump type 64, UV detector (variable-wavelength monitor), *EuroChrom 2000* integration package); *Knauer Lichrosolv Si-60*, 7- $\mu$ m column (250  $\times$  4 mm). Prep. HPLC: *Knauer* HPLC system (pump type 64, programmer 50, UV detector (variable-wavelength monitor)), or

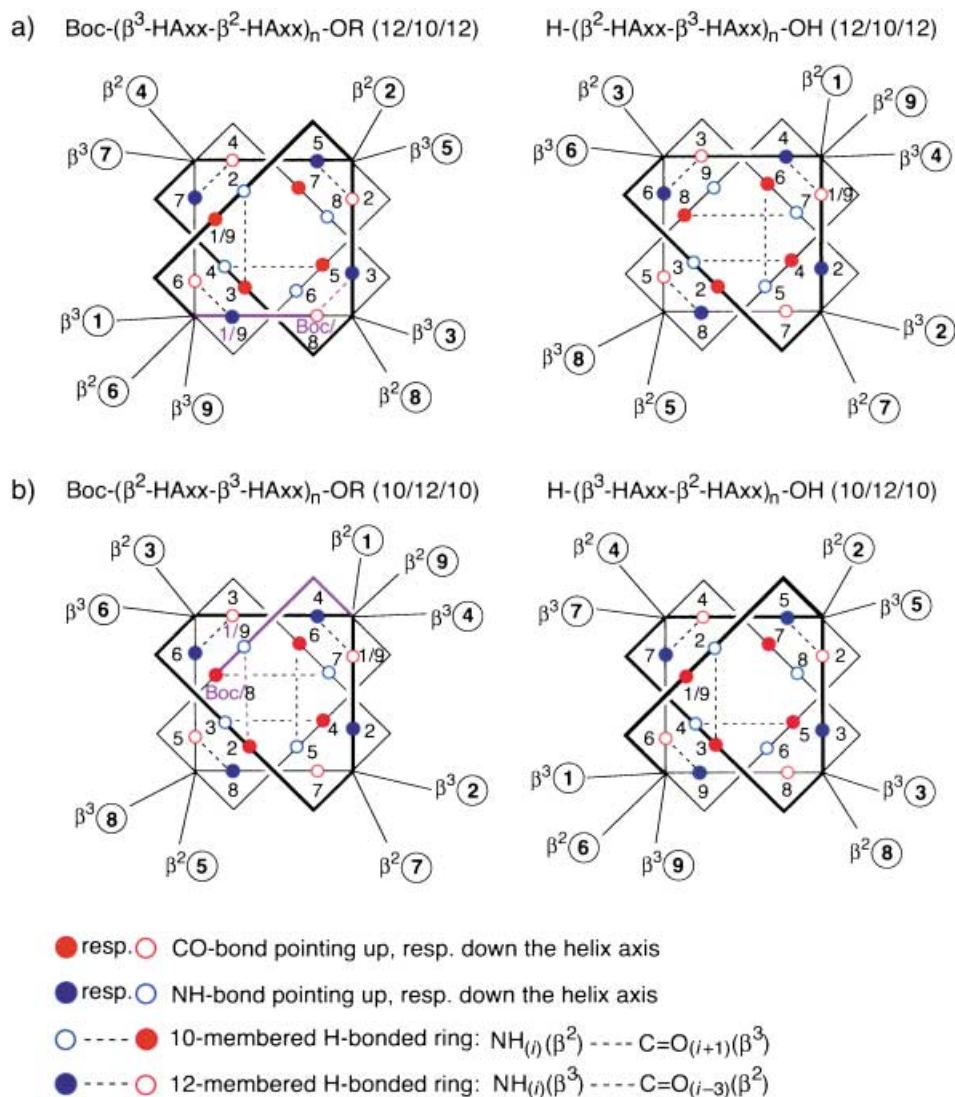


Fig. 7. Schematic representations of the right-handed 12/10- and 10/12-helical structures, looking down the helix axis from the N-termini. a) The Boc-protected  $\beta^3/\beta^2$ - and deprotected  $\beta^2/\beta^3$ -peptides form 12/10-helical structures. b) In contrast, Boc-protected  $\beta^3/\beta^3$ - and deprotected  $\beta^3/\beta^2$ -peptides form 10/12-helical structures. All helices are characterized by alternating twelve-membered H-bonded rings (from NH<sub>(i)</sub> of a  $\beta^3$ -amino acid residue to the C=O<sub>(i-3)</sub> of a  $\beta^2$ -amino acid residue, 'rectangular' route) and ten-membered H-bonded rings (from NH<sub>(i)</sub> of a  $\beta^2$ -amino acid residue to C=O<sub>(i+1)</sub> of a  $\beta^3$ -amino acid residue; 'suaric' route). The amide groups are pointing alternatively up and down the helix axis, and the C=O group of the Boc protecting group participates in the formation of the N-terminal H-bonded ring. The numbers 1–9 represent the positions of the  $\beta$ -amino acids in the nonapeptide sequence.

Merck HPLC system (*LaChrom*, pump type *L 7150*, UV detector *L 7400*, interface *D 7000*, HPLC Manager *D 7000*); *Knauer Lichrosolv Si-60*, 7-mm column (250 × 16 mm); TFA for prep. HPLC was used as UV-grade quality (> 99% GC). M.p.: *Büchi 510* apparatus; uncorrected. CD Spectra: *Jasco J-710* recording from 190 to 250 nm at r.t.; 1-mm rectangular cell; average of five scans, corrected for the baseline; peptide concentration 0.2 mM in MeOH; molar ellipticity  $\theta$  in deg·cm<sup>2</sup>·dmol<sup>-1</sup> ( $\lambda$  in nm); smoothing by *Jasco* software. IR Spectra: *Perkin-Elmer 782* spectrophotometer. NMR Spectra: *Bruker AMX-500* (<sup>1</sup>H: 500 MHz, <sup>13</sup>C: 125 MHz); chemical shifts  $\delta$  in ppm downfield from internal Me<sub>4</sub>Si (=0 ppm); *J* values in Hz. MS: *IonSpec Ultima 4.7 T FT Ion Cyclotron Resonance* (ICR; HR-MALDI, in 2,5-dihydroxybenzoic acid matrix) spectrometer; in *m/z* (% of basis peak).

2. *Benzyl Ester Deprotection: General Procedures 1 (GP 1)*. The fully protected oligopeptide was dissolved in MeOH (0.026–0.05M) and a cat. amount of Pd/C (10%) was added. The apparatus was evacuated, flushed three times with H<sub>2</sub>, and the mixture was stirred under H<sub>2</sub> for 20 h. Subsequent filtration through *Celite* and concentration under reduced pressure yielded the crude product, which was used without further purification.

3. *Boc Deprotection: General Procedure 2 (GP 2)*. The Boc-protected amino acid was dissolved in CH<sub>2</sub>Cl<sub>2</sub> or CHCl<sub>3</sub> (0.08–0.26M) and cooled to 0° (ice bath). An equal volume of TFA was added, and the mixture was allowed to slowly warm to r.t. and then stirred for a further 1.5–2 h. Concentration under reduced pressure and drying of the residue under h.v. (12 h) yielded the crude TFA salt, which was identified by NMR and used without further purification.

4. *Peptide Coupling with EDC: General Procedures 3 (GP 3)*. The appropriate TFA salt was dissolved in CHCl<sub>3</sub> (0.1–0.5M) and cooled to 0° (ice bath). This was treated successively with the Boc-protected fragment (1.3–2.9 equiv., added as solid or as a soln. in CHCl<sub>3</sub> (0.22M)), NMM (3.4–4.7 equiv.), HOBt (1.3–2.9 equiv.), and EDC (1.2–2.9 equiv.). The mixture was allowed to warm to r.t. and then stirred for 18–72 h. Subsequent dilution with CHCl<sub>3</sub> was followed by thorough washing with 1N HCl, sat. aq. NaHCO<sub>3</sub> soln., and sat. aq. NaCl soln. The org. phase was dried (MgSO<sub>4</sub>) and then concentrated under reduced pressure. FC or HPLC yielded the pure peptide.

5. *HPLC Analysis and Purification of  $\beta$ -Peptides. General Procedure 4 (GP 4)*. Normal-phase HPLC analysis was performed on a *Lichrosolv Si-60*, 7- $\mu$ m column (250 × 4 mm) with an isocratic mixture or a linear gradient of i-PrOH and hexane at a flow rate of 1 ml/min with UV detection at 220 nm. *t<sub>R</sub>* in min. Crude products were purified by prep. HPLC on a *Lichrosolv Si-60*, 7-mm column (250 × 21 mm) eluted with an isocratic mixture or a linear gradient of i-PrOH and hexane at a flow rate of 4 ml/min with UV detection at 220 nm and then evaporated under reduced pressure.

*Boc-(R)- $\beta^3$ -HVal-(S)- $\beta^2$ -HAla-(S)- $\beta^3$ -HLeu-OH (1b)*. Compound **1a** (0.14 g, 0.26 mmol) was transformed according to *GP 1* for 20 h in MeOH (10 ml) to yield **1b** (0.11 g, 99%), which was used without further purification.

*Boc-(R)- $\beta^3$ -HVal-(S)- $\beta^2$ -HAla-(S)- $\beta^3$ -HLeu-(S)- $\beta^2$ -HVal-(S)- $\beta^3$ -HAla-(S)- $\beta^2$ -HLeu-OBn (4a)*. Compound **2a** (41 mg, 77  $\mu$ mol) was Boc-deprotected in CH<sub>2</sub>Cl<sub>2</sub> (0.3 ml) according to *GP 2* for 1.5 h. The resulting TFA salt was treated at 0° (ice bath) with a soln. of **1b** (42 mg, 0.10 mmol) in CHCl<sub>3</sub> (0.6 ml), NMM (29  $\mu$ l, 0.26 mmol), HOBt (15 mg, 0.10 mmol), and EDC (18 mg, 95  $\mu$ mol) according to *GP 3* for 3 d. Purification by FC (MeOH/CH<sub>2</sub>Cl<sub>2</sub> 3:97) yielded **4a** (47 mg, 71%) with a purity of 86% (HPLC integration). For anal. purposes, **4a** was purified by HPLC (*Knauer* system, i-PrOH/hexane 7:93) according to *GP 4*. White solid. M.p. 221.5° (dec.). CD (0.2 mM in MeOH): +74.5 · 10<sup>4</sup> (202 nm); CD (0.2 mM in MeOH containing urea (3M)): +14.9 · 10<sup>4</sup> (211 nm). IR (KBr): 3290s, 3084w, 2960m, 2872w, 1734m, 1687s, 1647s, 1546s, 1457m, 1388m, 1367m, 1311m, 1251m, 1173m, 697w. <sup>1</sup>H-NMR (500 MHz, CD<sub>3</sub>OD): 0.87–0.93 (*m*, 7 Me); 0.97 (*d*, *J* = 6.7, Me); 1.02 (*d*, *J* = 6.8, Me); 1.17 (*d*, *J* = 6.7, Me); 1.24–1.31 (*m*, 2 CH); 1.44 (*s*, *t*-Bu); 1.51–1.59 (*m*, 3 CH); 1.66–1.80 (*m*, 3 CH); 1.89–1.93 (*m*, CH); 2.04–2.16 (*m*, 2 CH); 2.24–2.27 (*m*, CH); 2.31 (*dd*, *J* = 13.5, 7.8, 1 H, CH<sub>2</sub>); 2.41 (*dd*, *J* = 13.5, 5.5, 1 H, CH<sub>2</sub>); 2.57 (*dd*, *J* = 12.5, 3.4, 1 H, CH<sub>2</sub>); 2.61 (*dd*, *J* = 12.8, 3.4, 1 H, CH<sub>2</sub>); 2.72 (*dd*, *J* = 13.4, 10.4, 1 H, CH<sub>2</sub>); 2.75–2.81 (*m*, CH); 2.84 (*dd*, *J* = 13.1, 10.6, 1 H, CH<sub>2</sub>); 3.30–3.79 (*m*, 2 CH); 3.64 (*dd*, *J* = 13.4, 3.7, 1 H, CH<sub>2</sub>); 3.80 (*dd*, *J* = 13.2, 3.2, 1 H, CH<sub>2</sub>); 3.99–4.02 (*m*, CHN); 4.25–4.29 (*m*, CHN); 4.37–4.41 (*m*, CHN); 5.13 (*s*, CH<sub>2</sub>O); 6.43 (*d*, *J* = 10.3, NH); 7.29–7.38 (*m*, 5 arom. H). <sup>13</sup>C-NMR (125 MHz, CD<sub>3</sub>OD): 15.1, 18.5, 20.0, 20.7, 20.9, 21.4, 22.2, 22.5, 23.4, 23.8 (Me); 26.2, 27.3 (CH); 28.8 (Me); 29.3, 34.5 (CH); 40.4, 41.1, 41.5, 42.7 (CH<sub>2</sub>); 42.8 (CH); 43.7, 44.1 (CH<sub>2</sub>); 44.7 (CH); 44.9 (CH<sub>2</sub>); 45.1 (CH); 45.3 (CH<sub>2</sub>); 47.7, 55.1, 56.1 (CH); 67.5 (CH<sub>2</sub>); 80.1 (C); 129.3, 129.4, 129.6 (CH); 137.6, 158.6, 173.7, 174.3, 176.1, 176.2, 176.6 (C). HR-MALDI-MS: 881.5715 (2, [M + Na]<sup>+</sup>, C<sub>46</sub>H<sub>76</sub>N<sub>6</sub>NaO<sub>7</sub><sup>+</sup>; calc. 881.5728), 781.5192 (100, [M – Boc + Na]<sup>+</sup>, C<sub>41</sub>H<sub>70</sub>N<sub>6</sub>NaO<sub>7</sub><sup>+</sup>; calc. 781.5204), 759.5368 (7, [M – Boc + H]<sup>+</sup>, C<sub>41</sub>H<sub>71</sub>N<sub>6</sub>O<sub>7</sub><sup>+</sup>; calc. 759.5384).

*Boc-(R)- $\beta^3$ -HVal-(S)- $\beta^2$ -HAla-(S)- $\beta^3$ -HLeu-(S)- $\beta^2$ -HVal-(S)- $\beta^3$ -HAla-(S)- $\beta^2$ -HLeu-(R)- $\beta^3$ -HVal-(S)- $\beta^2$ -HAla-(S)- $\beta^3$ -HLeu-OBn (5a)*. Compound **3a** (33 mg, 38  $\mu$ mol) was Boc-deprotected in CH<sub>2</sub>Cl<sub>2</sub> (0.5 ml)

Table 5. *Weak* (w, 4.5 Å), *Medium* (m, 3.5 Å), and *Strong* (s, 3.0 Å) NOEs Observed in the ROESY NMR Spectra of Compound **3a** in MeOH

Residue	Atom	Residue	Atom	NOE	Residue	Atom	Residue	Atom	NOE
1	$\alpha$	1	$\delta$	s	1	NH	1	$\alpha$	w
1	$\alpha$	1	$\gamma$	m	1	NH	2	$\alpha$	w
1	$\alpha$	1	$\alpha'$	s	1	NH	1	$\alpha'$	m
1	$\alpha'$	1	$\gamma$	m	1	NH	1	$\gamma$	m
1	$\alpha'$	1	$\delta$	s	1	NH		$\text{tBu}$	w
2	$\alpha$	2	$\gamma$	s	1	NH	1	$\delta$	s
2	$\alpha$		$\text{tBu}$	m	2	NH	1	$\alpha$	s
2	$\alpha'$	2	$\gamma$	s	2	NH	5	$\alpha$	w
2	$\alpha'$	4	$\alpha$	w	2	NH	2	$\alpha$	w
3	$\alpha$	3	$\alpha'$	s	2	NH	1	$\alpha'$	m
3	$\alpha$	3	$\delta$	s	2	NH	4	$\alpha$	w
3	$\alpha$	3	$\varepsilon$	w	2	NH	3	$\varepsilon$	w
3	$\alpha$	3	$\gamma$	w	2	NH	3	$\beta$	w
3	$\alpha'$	3	$\gamma$	m	2	NH	1	$\beta$	s
3	$\alpha'$	3	$\varepsilon$	m	2	NH	4	$\beta$	w
4	$\alpha'$	4	$\gamma$	s	2	NH	2	$\beta$	w
4	$\alpha'$	4	$\delta$	w	2	NH	2	$\beta'$	s
5	$\alpha$	5	$\gamma$	s	2	NH	1	NH	w
5	$\alpha$	4	$\delta$	w	2	NH	3	NH	w
5	$\alpha'$	4	$\gamma$	m	3	NH	2	$\alpha$	s
5	$\alpha'$	4	$\delta$	m	3	NH	3	$\alpha'$	m
6	$\alpha$	6	$\gamma$	m	3	NH	3	$\gamma$	m
6	$\alpha$	6	$\varepsilon$	s	3	NH	3	$\delta$	m
1	$\beta$	1	$\alpha$	s	3	NH		$\text{tBu}$	w
1	$\beta$	2	$\alpha$	w	3	NH	2	$\alpha'$	w
1	$\beta$	3	$\alpha'$	s	3	NH	2	$\gamma$	w
1	$\beta$	1	$\gamma$	s	3	NH	3	$\beta$	m
1	$\beta$	3	$\gamma$	w	3	NH	1	$\beta$	m
1	$\beta$		$\text{tBu}$	w	3	NH	1	NH	w
1	$\beta$	1	$\delta$	s	3	NH	3	$\alpha$	w
2	$\beta$	2	$\alpha$	s	4	NH	3	$\alpha'$	w
2	$\beta$	2	$\gamma$	s	4	NH	3	$\beta$	s
3	$\beta$	3	$\alpha$	s	4	NH	4	$\beta$	w
3	$\beta$	5	$\alpha$	w	4	NH	6	$\beta$	w
3	$\beta$	5	$\alpha'$	m	4	NH	4	$\beta'$	s
3	$\beta$	3	$\alpha'$	m	4	NH	3	$\gamma$	w
3	$\beta$	4	$\alpha$	w	4	NH	3	$\alpha$	s
3	$\beta$	3	$\gamma$	m	5	NH	5	$\alpha$	m
3	$\beta$	3	$\delta$	m	5	NH	5	$\alpha'$	m
3	$\beta$	5	$\gamma$	w	5	NH	4	$\alpha$	s
3	$\beta$	2	$\gamma$	w	5	NH	4	$\gamma$	m
3	$\beta$	3	$\varepsilon$	s	5	NH	5	$\gamma$	s
4	$\beta$	4	$\alpha'$	s	5	NH	4	$\delta$	w
4	$\beta$	4	$\gamma$	m	5	NH	5	$\beta$	m
4	$\beta$	4	$\delta$	s	6	NH	5	$\alpha$	s
4	$\beta$	2	$\beta'$	m	6	NH	5	$\alpha'$	s
5	$\beta$	5	$\alpha$	s	6	NH	4	$\alpha$	w
5	$\beta$	5	$\alpha'$	s	6	NH	6	$\gamma$	w
5	$\beta$	4	$\alpha$	w	6	NH	5	$\gamma$	w
5	$\beta$	5	$\gamma$	s	6	NH	6	$\varepsilon$	w
5	$\beta$	4	$\delta$	w	6	NH	5	$\beta$	m
6	$\beta$	6	$\delta$	s	6	NH	6	$\beta$	s

Table 6. Weak (w, 4.5 Å), Medium (m, 3.5 Å), and Strong (s, 3.0 Å) NOEs Observed in the ROESY NMR Spectra of Compound **4a** in MeOH

Atom	Residue	Atom	Residue	NOE	Atom	Residue	Atom	Residue	NOE
NH	1	$\alpha$	3	m	NH	4	$\beta$	2	m
NH	1	$\beta$	3	w	NH	4	$\beta$	4	m
NH	1	$\alpha$	1	w	NH	4	$\beta$	1	w
NH	1	$\epsilon$	3	w	NH	4	$\beta$	3	m
NH	2	$\beta$	2	m	NH	4	$\alpha$	3	s
NH	2	$\beta$	1	w	NH	4	$\alpha$	4	s
NH	2	$\alpha$	2	w	NH	4	$\alpha$	4	m
NH	2	$\alpha$	1	s	NH	4	$\gamma$	4	m
NH	2	$\gamma$	1	m	$\beta$	4	$\alpha$	6	w
$\beta$	2	$\alpha$	2	m	$\beta$	4	$\alpha$	4	m
$\beta$	2	$\alpha$	4	w	$\beta$	4	$\delta$	4	m
NH	3	$\beta$	2	m	NH	5	$\beta$	6	w
NH	3	$\beta$	3	m	NH	5	$\beta$	4	m
NH	3	$\beta$	5	w	NH	5	$\beta$	5	m
NH	3	$\alpha$	2	s	NH	5	$\alpha$	4	s
NH	3	$\alpha$	5	w	NH	5	$\gamma$	5	w
NH	3	$\alpha$	4	w	NH	5	$\delta$	6	w
NH	3	Me	5	w	$\beta$	5	$\alpha$	4	w
$\beta$	3	$\alpha$	3	m	NH	6	$\beta$	6	m
$\beta$	3	$\gamma$	3	m	NH	6	$\beta$	4	m
$\gamma$	3	$\delta$	1	m	NH	6	$\beta$	5	m
$\beta$	3	$\alpha$	4	m	NH	6	$\alpha$	5	s
$\alpha$	3	$\gamma$	3	m	NH	6	$\gamma$	3	w
$\alpha$	3	$\beta$	3	m	NH	6	$\gamma$	6	m
$\gamma$	3	$\delta$	3	w	$\beta$	6	$\alpha$	6	m
NH	4	$\beta$	2	m	$\beta$	6	$\gamma$	6	w

according to *GP 2* for 2 h. The resulting TFA salt was treated at 0° (ice bath) with a soln. of **1b** (50 mg, 0.11 mmol) in CHCl<sub>3</sub> (0.5 ml), NMM (20  $\mu$ l, 0.18 mmol), HOBt (17 mg, 0.11 mmol), and EDC (22 mg, 0.11 mmol) according to *GP 3* to afford crude **5a** with a purity of 74% (HPLC integration). Purification by HPLC (Merck system, i-PrOH/hexane 5:95) according to *GP 4* yielded **5a** (13 mg, 29%). Colorless glass. HPLC (Knauer system, i-PrOH/hexane 6:94):  $t_R$  3.5, purity >99%.  $R_f$  (i-PrOH/hexane 1:9) 0.38. <sup>1</sup>H-NMR (500 MHz, CD<sub>3</sub>OH, solvent suppression by presaturation): 0.78–0.87 (*m*, 12 Me); 0.93–0.96 (*m*, 2 Me); 1.13 (*d*,  $J = 6.8$ , Me); 1.18–1.29 (*m*, 3 CH); 1.35 (*s*, *t*-Bu); 1.38–1.45 (*m*, 2 CH); 1.46–1.69 (*m*, 7 CH); 1.77–1.82 (*m*, CH); 1.95–2.11 (*m*, 4 CH); 2.15–2.19 (*m*, CH); 2.33–2.39 (*m*, CH); 2.40–2.47 (*m*, CH); 2.50–2.65 (*m*, 8 CH); 2.74–2.80 (*m*, CH); 3.38–3.43 (*m*, CH); 3.54–3.60 (*m*, CH); 3.81–3.86 (*m*, CH); 3.93–3.99 (*m*, CH); 4.13–4.19 (*m*, CH); 4.23–4.30 (*m*, CH); 4.44–4.53 (*m*, 3 CH);  $\nu_A = 4.98$ ,  $\nu_B = 5.09$  (*AB*,  $J_{AB} = 12.2$ , CH<sub>2</sub>O); 6.34 (*d*,  $J = 10.3$ , NH); 7.21–7.32 (*m*, 5 arom. H); 7.76–7.78 (*m*, NH); 8.14 (*d*,  $J = 9.5$ , NH); 8.39–8.48 (*m*, 5 NH); 8.78 (*d*,  $J = 9.8$ , NH). <sup>13</sup>C-NMR (125 MHz, CD<sub>3</sub>OH): 14.9; 15.2; 17.5; 18.4; 19.8; 20.1; 20.4; 21.0; 21.6; 21.8; 22.0; 22.1; 23.6; 23.6; 23.9; 25.9; 26.1; 27.1; 28.7; 42.0; 45.0; 54.6; 56.1; 67.7; 80.0; 129.2; 129.3; 129.4; 137.3; 158.5; 173.4; 173.7; 174.1; 174.2; 174.5; 175.6; 176.5; 176.7; 177.1. HR-MALDI-MS: 1106.7516 (100, [*M* – Boc + Na]<sup>+</sup>, C<sub>58</sub>H<sub>101</sub>N<sub>9</sub>NaO<sub>10</sub><sup>+</sup>; calc. 1106.7569).

*NMR Spectroscopy of 'mixed' peptides 3a–5a and 5d.* Sample: 6–8 mg dissolved in 0.6 ml of CD<sub>3</sub>OH. 1D-NMR (DRX500): <sup>1</sup>H-NMR (500 MHz): suppression of the CD<sub>3</sub>OH signal by presaturation; 90-K data points, 128 scans, 5.6-s acquisition time. [<sup>1</sup>H]-BB-decoupled <sup>13</sup>C-NMR (125 MHz): 80-K data points, 20-K scans, 1.3-s acquisition time, 1-s relax. delay, 45° excitation pulse. Processed with 1.0-Hz exponential line broadening. 2D-NMR: All with solvent suppression by presat. DQF-COSY (500 MHz, CD<sub>3</sub>OH) with pulsed-field gradients (PFG) for coherence pathway selection [39]: acquisition: 2K( $t_2$ )  $\times$  512 ( $t_1$ ) data points. 10 scans per  $t_1$  increment, 0.17-s acquisition time in  $t_2$ ; relaxation delay 2.0 s. TPPI Quadrature detection in  $\omega_1$ . Processing: zero filling and FT to 1K  $\times$  1K real/real data points after multiplication with sin<sup>2</sup> filter shifted by  $\pi/3$  in  $\omega_2$  and  $\pi/2$  in  $\omega_1$ . HSQC

Table 7. *Weak* (w, 4.5 Å), *Medium* (m, 3.5 Å), and *Strong* (s, 3.0 Å) NOEs Observed in the ROESY NMR Spectra of Compound **5a** in MeOH.

Atom	Residue	Atom	Residue	NOE	Atom	Residue	Atom	Residue	NOE
NH	1	$\alpha 1$	1	m	NH	5	$\beta$	5	m
NH	1	$\alpha 2$	1	w	NH	5	$\beta$	2	w
NH	1	$\gamma$	1	m	NH	5	$\alpha 2$	5	w
NH	1	$\beta$ u	1	m	NH	5	$\alpha$	4	s
NH	1	$\delta$	1	w	NH	5	$\gamma$	5	m
$\beta$	1	$\alpha 1$	1	m	$\beta$	5	$\alpha$	5	m
$\beta$	1	$\alpha 2$	3	m	$\beta$	5	$\alpha 2$	7	m
$\beta$	1	$\alpha 2$	1	w	$\beta$	5	$\gamma$	5	m
$\beta$	1	$\gamma$	1	m	NH	6	NH	7	w
$\beta$	1	$\beta$ u	1	w	NH	6	$\beta$	7	m
$\beta$	1	$\delta$	1	m	NH	6	$\beta$	6	w
NH	2	NH	3	w	NH	6	$\alpha$	8	w
NH	2	$\beta$	1	m	NH	6	$\alpha 2$	7	m
NH	2	$\beta$	2	w	NH	6	$\beta$	8	w
NH	2	$\beta$	4	w	NH	7	$\beta$	5	m
NH	2	$\alpha 2$	3	m	NH	7	$\beta$	7	m
NH	2	$\alpha 1$	1	m	NH	7	$\alpha$	6	s
NH	2	$\delta$	3	m	NH	7	$\alpha 2$	7	m
NH	2	$\epsilon$	3	w	NH	7	$\delta$	6	m
NH	3	$\beta$	3	m	$\beta$	7	$\alpha 2$	9	m
NH	3	$\beta$	1	m	$\beta$	7	$\alpha 1$	7	w
NH	3	$\alpha$	2	s	$\beta$	7	$\delta$	6	w
NH	3	$\alpha 2$	3	m	$\beta$	7	$\gamma$	6	w
NH	3	$\delta$	3	m	NH	8	NH	9	w
NH	3	$\beta$ u	1	m	NH	8	$\beta$	7	m
NH	3	$\epsilon$	3	w	NH	8	$\beta$	8	m
$\beta$	3	$\alpha 1$	3	m	NH	8	$\beta$	8	w
$\beta$	3	$\alpha 2$	5	w	NH	8	$\alpha 2$	9	m
$\beta$	3	$\delta$	3	w	NH	9	$\beta$	9	m
$\beta$	3	$\gamma$	3	w	NH	9	$\beta$	7	m
$\beta$	3	$\gamma$	3	m	NH	9	$\alpha$	9	m
$\beta$	3	$\epsilon$	3	w	NH	9	$\alpha$	8	m
NH	4	$\beta$	3	m	$\beta$	9	$\alpha$	9	m
NH	4	$\beta$	4	m	$\beta$	9	$\delta$	9	w
NH	4	$\beta$	6	w	$\beta$	9	$\gamma$	9	w
NH	4	$\alpha 2$	3	s	$\beta$	9	$\gamma$	9	m
NH	4	$\alpha$	4	m	$\beta$	9	$\epsilon$	9	w

with PFG [40] (500, 125 MHz, CD<sub>3</sub>OH): acquisition: 2K( $t_2$ )  $\times$  512 ( $t_1$ ) data points, 48 scans per  $t_1$  increment. <sup>13</sup>C-GARP decoupling during  $t_2$ . 0.17-s acq. time in  $t_2$ . Processing: zero filling and FT to 1K  $\times$  1K real/real data points after multiplication with sin<sup>2</sup> filter shifted by  $\pi/2$  in  $\omega_2$  and sin filter shifted by  $\pi/2$  in  $\omega_1$ . HMBC with PFG [41] (500, 125 MHz, CD<sub>3</sub>OH): acquisition: delay for evolution of long-range antiphase magn. 50 ms. No <sup>13</sup>C-decoupling, otherwise identical to parameters for HSQC. Processing: zero filling and FT to 1K  $\times$  1K after multiplication with cos<sup>2</sup> filter in  $\omega_2$  and Gaussian filter in  $\omega_1$ ; power spectrum in both dimensions. ROESY [42] (500 MHz, CD<sub>3</sub>OH) (see Tables 5–8). Acquisition: 2 ROESY spectra with mixing times of 150 and 300 ms were acquired. CW-spin lock (2.7 kHz) between trim pulses, 2K( $t_2$ )  $\times$  512 ( $t_1$ ) data points, 64 scans per  $t_1$  increment. 0.17-s acq. time in  $t_2$ , other parameters identical to DQF-COSY. Processing: zero filling and FT to 1K  $\times$  512K real/real data points after multiplication by cos<sup>2</sup> filter in  $\omega_2$  and  $\omega_1$ . Baseline correction with 3rd degree polynomial in both dimensions.

Table 8. Weak (w, 4.5 Å), Medium (m, 3.5 Å), and Strong (s, 3.0 Å) NOEs Observed in the ROESY NMR Spectra of Compound **5d** in MeOH

Atom	Residue	Atom	Residue	NOE	Atom	Residue	Atom	Residue	NOE
$\beta$	1	$\alpha 1$	1	m	NH	6	$\beta$	6	m
$\beta$	1	$\alpha 2$	1	w	NH	6	$\beta$	6	w
$\beta$	1	$\alpha 2$	3	m	NH	6	$\alpha 1$	8	w
$\beta$	1	$\gamma$	1	m	NH	7	$\beta$	5	m
$\beta$	1	$\delta$	1	w	NH	7	$\beta$	7	m
NH	2	NH	3	w	NH	7	$\alpha 2$	7	w
NH	2	$\beta$	2	w	NH	7	$\delta$	7	w
NH	2	$\beta$	2	m	NH	7	$\gamma$	7	m
NH	2	$\alpha 1$	1	m	$\beta$	7	$\alpha 1$	7	m
NH	2	$\alpha 2$	1	m	$\beta$	7	$\gamma$	7	m
NH	3	$\beta$	3	m	$\beta$	7	$\alpha 2$	9	w
NH	3	$\alpha$	2	s	NH	8	NH	9	w
NH	3	$\alpha$	3	m	NH	8	$\beta$	7	m
NH	3	$\gamma$	3	m	NH	8	$\beta$	8	w
NH	3	$\delta$	3	w	NH	8	$\beta$	8	m
NH	3	$\epsilon$	3	w	NH	8	$\alpha 2$	9	m
$\beta$	3	$\alpha 1$	3	m	NH	8	$\alpha 1$	7	w
$\beta$	3	$\alpha 2$	5	m	NH	9	$\beta$	9	m
$\beta$	3	$\gamma$	3	m	NH	9	$\beta$	7	m
$\beta$	3	$\gamma$	3	m	NH	9	$\alpha$	8	s
$\beta$	3	$\delta$	3	w	NH	9	$\alpha 2$	9	m
$\beta$	3	$\epsilon$	3	m	NH	9	$\gamma$	9	m
NH	4	$\beta$	4	m	NH	9	$\gamma$	9	w
NH	4	$\beta$	4	m	NH	9	$\delta$	9	w
NH	4	$\alpha 1$	5	m	NH	9	$\epsilon$	9	w
NH	4	$\alpha 2$	5	w	$\beta$	9	$\alpha 1$	9	m
NH	5	$\beta$	3	w	$\beta$	9	$\delta$	9	w
NH	5	$\alpha$	4	m	$\beta$	9	$\gamma$	9	m
NH	5	$\alpha 2$	5	m	NH	2	$\beta$	5	w
NH	5	$\gamma$	5	m	NH	6	$\beta$	3	w
$\beta$	5	$\alpha 1$	5	m	NH	6	$\beta$	4	w
$\beta$	5	$\alpha 2$	7	m					
$\beta$	5	$\gamma$	5	m					
NH	6	$\beta$	7	w					

*NMR Structure Determination:* Calculations were performed according to the X-PLOR protocol [43] on a Silicon Graphics Octane workstation under Irix 6.5. Visualization was carried out with MolMol [44] (see Figs. 3–6). The simulated annealing protocol X-PLOR of Quanta 2000 (Accelrys Inc., San Diego) was used to generate the structures starting from randomized conformations. Initial temp.: 800 K, 4000 high steps, 2000 cooling steps, 1.5-fs time step, all other parameters were left unchanged. The resulting structures converged to a right-handed helical structure. A final refinement with the slow-cooling simulated annealing protocol, starting temp. 300 K, 1-ps time step and, energy minimization yielded lowest energy structures, which are depicted in Figs. 3–6. We took these structures as representatives for the conformation in MeOH solution. NOEs that are not compatible with the 12/10-helical structure for the deprotected  $\beta$ -peptide **5d** were not considered in the calculation.

## REFERENCES

- [1] D. J. Hill, M. J. Mio, R. B. Prince, T. S. Hughes, J. S. Moore, *Chem. Rev.* **2001**, *101*, 3893.
- [2] D. Seebach, J. L. Matthews, *Chem. Commun.* **1997**, 2015.



- [3] S. H. Gellman, *Acc. Chem. Res.* **1998**, *31*, 173.
- [4] W. F. DeGrado, J. P. Schneider, Y. Hamuro, *J. Pept. Res.* **1999**, *54*, 206.
- [5] K. Gademann, T. Hintermann, J. V. Schreiber, *Curr. Med. Chem.* **1999**, *6*, 905.
- [6] R. P. Cheng, S. H. Gellman, W. F. DeGrado, *Chem. Rev.* **2001**, *101*, 3219.
- [7] D. Seebach, M. Overhand, F. N. M. Kühnle, B. Martinoni, L. Oberer, U. Hommel, H. Widmer, *Helv. Chim. Acta* **1996**, *79*, 913.
- [8] D. Seebach, P. E. Ciceri, M. Overhand, B. Jaun, D. Rigo, L. Oberer, U. Hommel, R. Amstutz, H. Widmer, *Helv. Chim. Acta* **1996**, *79*, 2043.
- [9] D. H. Appella, L. A. Christianson, I. L. Karle, D. R. Powell, S. H. Gellman, *J. Am. Chem. Soc.* **1996**, *118*, 13071.
- [10] T. Sifferlen, M. Rueping, K. Gademann, B. Jaun, D. Seebach, *Helv. Chim. Acta* **1999**, *82*, 2067.
- [11] D. H. Appella, L. A. Christianson, I. L. Karle, D. R. Powell, S. H. Gellman, *J. Am. Chem. Soc.* **1999**, *121*, 6206.
- [12] D. Seebach, A. Jacobi, M. Rueping, K. Gademann, M. Ernst, B. Jaun, *Helv. Chim. Acta* **2000**, *83*, 2115.
- [13] M. Rueping, B. Jaun, D. Seebach, *Chem. Commun.* **2000**, 2267.
- [14] J. J. Barchi, X. L. Huang, D. H. Appella, L. A. Christianson, S. R. Durell, S. H. Gellman, *J. Am. Chem. Soc.* **2000**, *122*, 2711.
- [15] D. H. Appella, P. R. LePlae, T. L. Raguse, S. H. Gellman, *J. Org. Chem.* **2000**, *65*, 4766.
- [16] P. I. Arvidsson, M. Rueping, D. Seebach, *Chem. Commun.* **2001**, 649.
- [17] T. Etezady-Esfarjani, C. Hilty, K. Wüthrich, M. Rueping, J. V. Schreiber, D. Seebach, *Helv. Chim. Acta* **2002**, *85*, 1197.
- [18] D. H. Appella, L. A. Christianson, D. A. Klein, D. R. Powell, X. L. Huang, J. J. Barchi, S. H. Gellman, *Nature* **1997**, *387*, 381.
- [19] D. H. Appella, L. A. Christianson, D. A. Klein, M. R. Richards, D. R. Powell, S. H. Gellman, *J. Am. Chem. Soc.* **1999**, *121*, 7574.
- [20] T. D. W. Claridge, J. M. Goodman, A. Moreno, D. Angus, S. F. Barker, C. Taillefumier, M. P. Watterson, G. W. J. Fleet, *Tetrahedron Lett.* **2001**, *42*, 4251.
- [21] S. Abele, P. Seiler, D. Seebach, *Helv. Chim. Acta* **1999**, *82*, 1559.
- [22] D. Seebach, K. Gademann, J. V. Schreiber, J. L. Matthews, T. Hintermann, B. Jaun, L. Oberer, U. Hommel, H. Widmer, *Helv. Chim. Acta* **1997**, *80*, 2033.
- [23] D. Seebach, S. Abele, K. Gademann, G. Guichard, T. Hintermann, B. Jaun, J. L. Matthews, J. V. Schreiber, *Helv. Chim. Acta* **1998**, *81*, 932.
- [24] D. Seebach, S. Abele, K. Gademann, B. Jaun, *Angew. Chem., Int. Ed.* **1999**, *38*, 1595.
- [25] K. Gademann, T. Kimmerlin, D. Hoyer, D. Seebach, *J. Med. Chem.* **2001**, *44*, 2460.
- [26] D. Seebach, M. Rueping, P. I. Arvidsson, T. Kimmerlin, P. Micuch, C. Noti, D. Langenegger, D. Hoyer, *Helv. Chim. Acta* **2001**, *84*, 3503.
- [27] Y. D. Wu, D. P. Wang, *J. Am. Chem. Soc.* **1998**, *120*, 13485.
- [28] Y. D. Wu, D. P. Wang, *J. Am. Chem. Soc.* **1999**, *121*, 9352.
- [29] K. Möhle, R. Gunther, M. Thormann, N. Sewald, H. J. Hofmann, *Biopolymers* **1999**, *50*, 167.
- [30] X. Daura, K. Gademann, B. Jaun, D. Seebach, W. F. van Gunsteren, A. E. Mark, *Angew. Chem., Int. Ed.* **1999**, *38*, 236.
- [31] D. Seebach, J. V. Schreiber, S. Abele, X. Daura, W. F. van Gunsteren, *Helv. Chim. Acta* **2000**, *83*, 34.
- [32] J. Podlech, D. Seebach, *Liebigs Ann.* **1995**, 1217.
- [33] J. Podlech, D. Seebach, *Angew. Chem., Int. Ed.* **1995**, *34*, 471.
- [34] T. Hintermann, D. Seebach, *Synlett* **1997**, 437.
- [35] T. Hintermann, D. Seebach, *Helv. Chim. Acta* **1998**, *81*, 2093.
- [36] C. Gaul, B. Schweizer, P. Seiler, D. Seebach, *Helv. Chim. Acta* **2002**, *85*, 1546.
- [37] N. Berova, K. Nakanishi, R. W. Woody, 'Circular Dichroism, Principles and Application', Wiley-VCH, 2000.
- [38] J. J. Cheng, T. J. Deming, *Macromolecules* **2001**, *34*, 5169.
- [39] A. L. Davis, E. D. Laue, J. Keeler, D. Moskau, J. Lohman, *J. Magn. Reson.* **1991**, *94*, 637.
- [40] A. L. Davis, J. Keeler, E. D. Laue, D. Moskau, *J. Magn. Reson.* **1992**, *98*, 207.
- [41] W. Willker, D. Leibfritz, R. Kerssebaum, W. Bermel, *Magn. Reson. Chem.* **1993**, *31*, 287.
- [42] C. Griesinger, R. R. Ernst, *J. Magn. Reson.* **1987**, *75*, 261.
- [43] A. T. Brünger, in 'X-PLOR Manual V3.0', Yale University, New Haven, 1992.
- [44] R. Koradi, M. Billeter, K. Wüthrich, *J. Mol. Graph.* **1996**, *14*, 51.

Received July 3, 2002